Formation and Propagation of a Proton Ring

P. L. Dreike,[a] J. B. Greenly, D. A. Hammer, and R. N. Sudan
Laboratory of Plasma Studies, Cornell University, Ithaca, New York 14853
(Received 4 August 1980)

A magnetically self-confined ring of 430-keV protons with a field reversal on axis of 3% is formed in an 8-kG solenoid, as evidenced by propagation more than 1 m in 15–400 mTorr air or hydrogen without dispersion. Up to 83% of the proton kinetic energy is in rotation and inductive coupling of axial ring energy to azimuthal plasma current induced in air (but not hydrogen) gives reflection of >50% of the ring from a 23% mirror.

PACS numbers: 52.55.Ke

Magnetic field configurations in which an externally applied magnetic field is reversed by currents flowing in the plasma itself are expected to have favorable plasma confinement properties and have, therefore, attracted considerable interest for fusion reactors. The current may be carried by either low-energy plasma particles or by rings of high-energy particles. Synchrotron radiation losses by energetic electrons, the possibility of plasma heating by the energetic ions,[1] and theoretical predictions of a more stable configuration[2] have lead to field-reversal schemes with use of high-energy ions. Recent developments in intense ion-beam technology have made it possible to attempt single-pulse injection and trapping of a field-reversing proton ring in a mirror well on a time scale of 0.1–1.0 μsec. Indeed, the transient reversal of an applied magnetic field by a rotating proton beam has recently been reported,[3] although the average axial velocity and its dispersion are too large for the beam to be trapped in a mirror well or confined in its own diamagnetic well.

In this Letter we report experimental results on the formation and dynamics of a rotating proton ring, whose quality is such that particles are trapped in their own 3% diamagnetic well. To summarize, an annular ~430-keV proton beam from a magnetically insulated diode is injected through a cusplike magnetic field to form a rotating proton beam. With $\gtrsim$ 15 mTorr air or $\gtrsim$ 50 mTorr H_2 in the experiment chamber, up to 83% of the total kinetic energy of the ring is in rotation, and the axial energy dispersion of the protons with enough energy to traverse the cusp is sufficiently small so that >70% are held together axially by their own 3% diamagnetic well as they propagate more than 1 m in an 8-kG solenoidal magnetic field. Up to 15% of the residual axial beam energy is inductively coupled to azimuthal plasma currents induced in the beam-generated plasma in air, but such currents are not observed in hydrogen. Consequently, the proton beams are more efficiently reflected from the 1.23-mirror-ratio downstream mirror in air than in hydrogen, with $\gtrsim$ 50% achieved in air. About 1% inductive energy coupling to wall resistors was observed in both air and hydrogen experiments.

A schematic drawing of the apparatus is shown in Fig. 1(a). The 2.5-m-long solenoid is operated at 8 kG in the experiments reported here. The proton source is an annular magnetically insulated diode, similar to one described previously.[4] Pulsed coils within the anode of the diode provide both closed magnetic-flux surfaces around the anode which insulate against electron flow and a cusplike transition to the solenoidal field, as shown in Fig. 1(b). The diode is powered by a 90-nsec, 550-kV, 90-kA pulse. The annular proton beam is injected through a 2-μm-thick Mylar

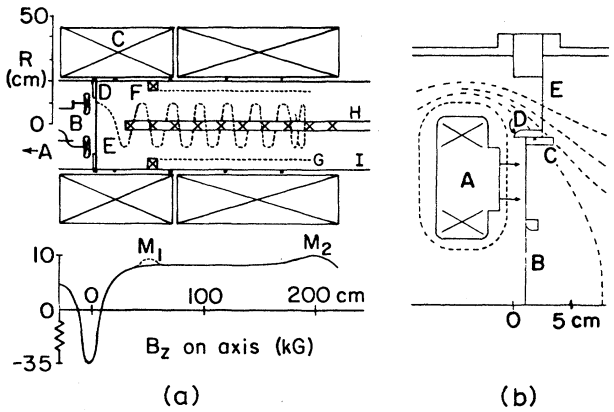

FIG. 1. (a) Schematic: *A*, to the Neptune generator; *B*, anode; *C*, external coils; *D*, cathode, including 2 μm Mylar foil; *E*, typical proton orbit; *F*, upstream mirror coil; *G*, wall resistor wires; *H*, axis diagnostic assembly with pickup loops; *I*, vacuum chamber wall. Also shown is the total magnetic field at $r=0$ with the upstream mirror field dashed. (b) Diode detail: *A*, anode with coils; *B*, cathode foil; *C*, cathode foil holder; *D*, cathode edge for electron emission; *E*, cathode ground return. Field lines shown dashed.

foil, with about 130 keV energy loss, into a drift chamber containing 15–400 mTorr of neutral gas to provide space-charge neutralization. The radial component of the cusp field converts beam energy to rotation as the beam drifts to the uniform field section. The ring then propagates about 2 m to the fixed 1.23 downstream mirror, M_2, where it is partially reflected. Mirror M_1, necessary for ring trapping if sufficient axial energy can be removed from the ring, is produced by a pulsed coil within the vacuum vessel. The ring may lose axial energy by inductive coupling to plasma return currents or to an array of resistor wires located between 70 and 190 cm from the diode. The diagnostics used in these experiments are (1) ten fast magnetic pickup loops to measure magnetic field changes on the axis at 20 cm intervals from 32 to 212 cm from the diode, (2) magnetically insulated Faraday cups oriented to measure the rotating proton flux, (3) four miniature Rogowski belts to measure the current induced in four of the wall resistor wires, (4) magnetic probes outside the ring oriented to measure axial and azimuthal magnetic fields of the ring, and (5) Thermofax paper witness targets to measure the radial extent of the ring.

The magnetic field configuration near the diode [Fig. 1(b)] is such that the anode emission surface is nearly coincident with a magnetic-flux surface. This minimizes the spread of the particles' initial canonical angular momenta and, therefore, their spread in axial velocities after traversing the cusp (if we assume azimuthal symmetry and space-charge neutralization). Furthermore, the radial component of the Lorentz force on the protons is always directed inward which minimizes the radial loss of ions in traversing the cusp when the magnetic field is near the cusp transmission limit.[5] When the drift chamber is pressurized to a few tens of millitorr of air, hydrogen, helium, or nitrogen, the beam is space-charge neutralized by the beam-generated plasma, and a clearly defined hollow ring is produced which propagates through the system with little radial spreading and with $\gtrsim 80\%$ of its energy in the transverse direction. Thermofax paper witness targets show its mean radius is 10 cm and its thickness is 6 cm. When the beam is injected into vacuum ($\lesssim 10^{-3}$ Torr), it is radially and axially dispersed on a $\frac{1}{2}$ m distance scale, despite the presence of surface flashover electron sources in the cusp region, as previously used,[4] indicating inadequate space-charge neutralization in the cusp.

Proton beam dynamics in the magnetic mirror region are a strong function of the gas species and a weak function of pressure. A lower bound on the beam-generated plasma density is obtained by considering only impact ionization by the fast protons. With use of tabulated cross sections,[6] plasma densities of about 4×10^{12} and 1.5×10^{13} cm^{-3} are produced by the 25-A/cm^2 (1.7×10^{11} cm^{-3}) beam in 100 mTorr of hydrogen and air, respectively. Ionization by secondaries and avalanching in the induced electric fields of the beam will surely cause these densities to be substantially higher. Null measurements of azimuthal magnetic fields show that the ring is (90–100)% *axially* current neutralized by induced plasma currents. *Azimuthal* plasma currents, on the other hand, are observed only in the heavier gases—air, nitrogen, and helium—but not in hydrogen or deuterium. Three plasma current "signatures" are seen: The magnetic signals (1) persist after passage of the high-energy protons, (2) are often flat topped, evidently because the plasma current starts to flow as some critical plasma condition is reached, and (3) are pressure dependent. The rotating proton flux is measured using small Faraday cups (magnetically insulated by the solenoidal field) at various axial positions, and at 10 cm radius, with their axes oriented in the azimuthal direction. The cups' apertures were covered with 2-μm-thick Mylar foil to discriminate against low-energy particles, and the pressure inside the cups was maintained at 0.1 mTorr. Faraday cup and axis diamagnetic signals at the same axial positions are compared in Fig. 2 for shots into 240 mTorr hydrogen and 230 mTorr air. There is good correspondence between the two for a hydrogen fill. Moreover, the magnetic signal amplitudes and widths are independent of pressure in hydrogen. However, in air the magnetic signals are much longer than the particle

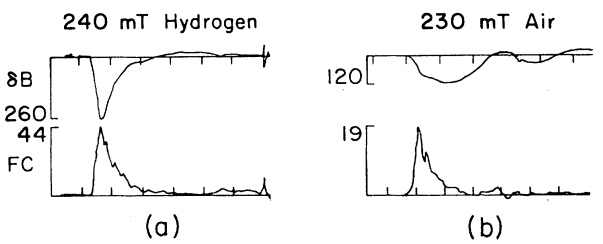

FIG. 2. Beam diamagnetism and Faraday cup measurements of the rotating proton flux for (a) in 240 mTorr H_2 and (b) in 230 mTorr air. The time sweep is 200 nsec/div and the Faraday-cup signal is in A/cm^2.

flux signals and they tend to be flat topped at pressures > 100 mTorr. The duration of their tails increases with the square root of the fill pressure, and they oscillate at low pressures, $\lesssim$ 30 mTorr. This plasma current behavior as a function of ion mass is as predicted theoretically for the similar problem of return currents induced by a rotating electron beam in a plasma in an axial magnetic field by Lee and Sudan[7] and by Chu and Rostoker.[7] To summarize, the hydrogen ions can undergo drift motion in response to the ring electric fields on the time scale of beam transit, but the heavier ions cannot. Therefore, net plasma currents can flow only in the heavier-ion plasmas.

Oscillographs of the ring's diamagnetism at three different axial positions for a shot into 320 mTorr hydrogen are reproduced in Fig. 3(a) together with the diode voltage and current histories for this shot in Fig. 3(b). The average injected proton energy is 430 keV during the 60-nsec usable portion of the pulse, corresponding to a total velocity of 9.1×10^8 cm/sec. The ring propagates with an axial velocity of 3.8×10^8 cm/sec, corresponding to an average axial energy of $\bar{W}_z$ = 75 keV. Within 10%, the magnitude of the diamagnetism is 225 G and the full width at half maximum is 100 nsec at all probe positions between 72 and 172 cm. This implies an axial energy spread of $\Delta W_z \lesssim$ 15 keV since protons with larger ring frame energies would not be confined by the 3% magnetic well produced by the ring. (The alternative explanation of an axial energy dispersion of $\lesssim$ 0.2 keV is not reasonable.) Because the inferred ratio of total particle kinetic energy to perpendicular energy is $1.21\pm0.07\approx M_2 = 1.23$, a

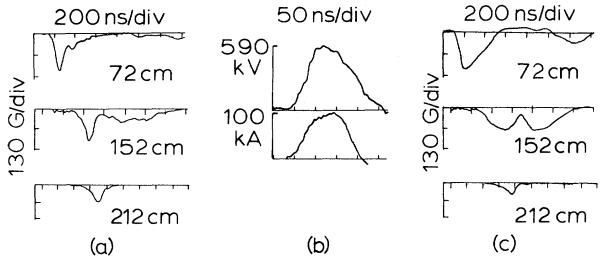

FIG. 3. (a) Ring diamagnetism at three axial positions for a shot in 320 mTorr H_2. (b) Diode voltage and current waveforms for the shot of (a). (c) Ring diamagnetism at the same positions for a similar shot in 140 mTorr air. The 72- and 152-cm signals are time synchronized at the right-hand side, but the 212-cm signal is not.

fraction of the ring is expected to reflect from M_2. Indeed, the long tails on the diamagnetic signals at 72 and 152 cm are due to particles which are too slow to be contained in the main ring, and which reflect from M_2. This interpretation is supported by (1) the absence of a tail at 212 cm, implying a transmission cutoff, (2) backward propagation of tail features which can be seen in full sets of diamagnetic signals from 32 to 192 cm, and (3) negligible tails for shots with M_1 > 10%, for which the slowest particles are reflected at 50–55 cm, i.e., before they enter the mirror region.

The total charge and energy in the ring can be estimated from the diamagnetic signals with use of a solenoid model for the ring and its measured axial velocity. One obtains $Q_p = (0.9\pm0.3)\times10^{-3}$ C or $(5.5\pm2)\times10^{15}$ total protons. The corresponding energy is 380 J, with an axial energy of 65 J.

Oscillographs of the ring diamagnetism from a similar shot into a 140-mTorr air fill are reproduced in Fig. 3(c). Because of the plasma currents, the diamagnetic signals in air are smaller and have longer durations than those in hydrogen. The second peak is due to reflection of the ring from M_2, as seen from the direction of propagation, and the considerably reduced diamagnetism at 212 cm. Rings were consistently reflected in an air fill, while a coherent ring reflection in hydrogen was rarely observed. This is attributed to transfer of some of the ring's axial energy to the magnetic energy of the plasma currents.[7] For a typical shot with δB = 200 G, nearly 10 J of the 65 J of axial energy is left behind in the ~10-cm-radius, 1.5-m-long return-current configuration. Within bounds allowed by the presence of plasma currents, comparison of the incident and reflected diamagnetic signals at 152 cm and the transmitted signal at 212 cm suggest > 50% reflection of ring protons. The gradual loss of particles in the reflected ring, exemplified by the 152- and 72-cm traces in Fig. 3(c), has an inverse pressure dependence and is not explained by classical binary collisions or charge exchange with background neutrals.

Three other noteworthy observations have been made. First, measurements of the current induced in the resistor wires showed that up to 1% of the ring's axial energy was dissipated in the wires in agreement with models of this mechanism.[8,9] Second, a peak ring diamagnetism of 875 G ± 10% was observed 50 cm from the diode with M_1 = 1.25. Note that our peak diode power is only 0.05 TW. Third, ring trajectories as a function

of diode voltage are in good agreement with the calculated orbits of typical single particles.

In summary, an ion source giving sufficient beam quality for self-confined ring formation has been developed. Axial energy has been extracted from the ring by two collective interactions, with return currents and with a resistive wall. Finally, the ring has been reflected from a weak mirror. Based upon these observations, the theoretical scaling of energy dissipation in a resistive wall,[9] and extensive computer simulations,[8] it is expected that a proton ring can be trapped if the injected proton current is increased by a factor of 3–4, the resistive wall is optimized, and the shape of mirror region is modified.

This work was supported by the U. S. Department of Energy under Contract No. DE-AS02-77ET53005.

[a]Permanent address: Sandia Laboratories, Albuquerque, New Mexico 87185.

[1]N. C. Christofilos, U. S. Patent No. 3 664 921 (1972).

[2]R. V. Lovelace, Phys. Rev. Lett. 35, 162 (1975); R. N. Sudan and M. N. Rosenbluth, Phys. Rev. Lett. 36, 972 (1976).

[3]C. A. Kapetanakos, J. Golden, J. A. Pasour, S. J. Marsh, and R. A. Mahaffey, Phys. Rev. Lett. 44, 1218 (1980).

[4]P. L. Dreike, D. A. Hammer, R. N. Sudan, and L. G. Wiley, Phys. Rev. Lett. 41, 1328 (1978).

[5]M. J. Rhee and W. W. Destler, Phys. Fluids 17, 1574 (1974).

[6]Example, E. W. McDaniel, *Collision Phenomena in Ionized Gases* (Wiley, New York, 1964), pp. 182–189.

[7]R. Lee and R. N. Sudan, Phys. Fluids 13, 2621 (1970); K. R. Chu and N. Rostoker, Phys. Fluids 17, 813 (1974).

[8]A. Mankofsky, A. Friedman, and R. N. Sudan, to be published.

[9]D. J. Rej, D. A. Larrabee, and H. H. Fleischmann, J. Appl. Phys. 51, 5285 (1980).

Bounds on the Electromagnetic, Elastic, and Other Properties of Two-Component Composites

G. W. Milton

Department of Theoretical Physics, The University of Sydney, Sydney, New South Wales 2006, Australia

(Received 29 September 1980)

A simple relation between three-point correlation functions is derived for two-component materials. This relation enables one to find concise expressions for the Beran, Molyneux, and McCoy bounds on transport and elastic coefficients in terms of the volume fraction, f_1, and two fundamental geometric parameters, ζ_1 and η_1. The parameter ζ_1 also determines bounds on the complex electrical permittivity. No simple interpretation of ζ_1 and η_1 has been found.

PACS numbers: 62.20.Dc, 72.15.Eb, 78.20.Dj

This work is concerned with estimating the transport and elastic properties of a macroscopically homogeneous and isotropic composite, given the transport and elastic properties of the two components. Once a relation is found for any one transport coefficient it applies to any other transport coefficient. Indeed finding the effective electrical conductivity, heat conductivity, magnetic permeability, or diffusivity is mathematically analogous[1] to finding the effective electrical permittivity, ϵ_e, given the permittivities, ϵ_1 and ϵ_2 of the components.

The effective thermal expansion coefficient and consequently the specific heats of the composite can also be determined,[2,3] once we have found the effective bulk modulus, κ_e, and the effective shear modulus, μ_e, in terms of the bulk moduli, κ_1 and κ_2, and the shear moduli, μ_1 and μ_2, of the components. Furthermore[4] the work of Goodier[5] relates the effective viscosity of a composite (such as a suspension of particles in a fluid) to μ_e for a composite of incompressible materials (such as a suspension of particles in a solid matrix). Because of these relations, I focus on finding ϵ_e, κ_e, and μ_e, given ϵ_1, ϵ_2, κ_1, κ_2, μ_1, μ_2, and information about the structure of the material, including the volume fractions, f_1 and $f_2 = 1 - f_1$, of the components.

Beran, Molyneux, and McCoy[6-8] have derived bounds on ϵ_e, κ_e, and μ_e which provide both an estimate of each quantity and the uncertainty associated with the estimate. They assume that the scale of inhomogeneities is much larger than atomic dimensions and that the composite is free

